

# Formation of Polyamide 12–Polyisoprene Core–Shell Particles in Polystyrene by Reactive Blending

C. Koulic,<sup>†</sup> G. François, and R. Jérôme\*

Center for Education and Research on Macromolecules (CERM), University of Liège (ULg),  
B6 Sart Tilman, B-4000 Liège, Belgium

Received December 4, 2003; Revised Manuscript Received March 29, 2004

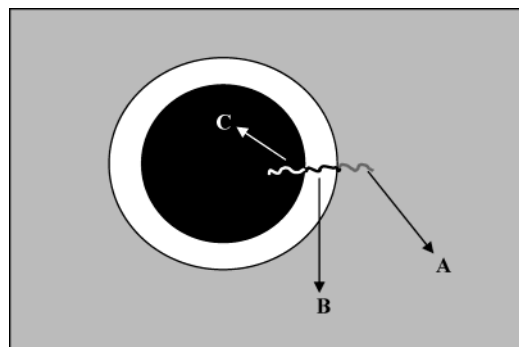
**ABSTRACT:** Polyamide 12 (PA12)–polyisoprene (PIP) particles with a thermoplastic core and a rubbery shell have been prepared in a thermoplastic matrix (PS) by reactive blending. For this purpose, an anhydride-end-capped PS-*b*-PIP diblock (PS-*b*-PIP-anh) has been reacted with PA12 chains end-capped (50% of them) by a primary amine and dispersed in PS. A PS-*b*-PIP-PA12 triblock has been formed at the interface between the PS matrix and the dispersed PA12 microdomains. Thus, the phase morphology consists of PA12 core–PIP shell particles dispersed in PS. The nonreacted PA12 with respect to PS-*b*-PIP-anh dictates the size of the polyamide (core) domains, and the reactive diblock (mainly the molecular weight of the PIP block) imposes the shell thickness and modulates the core size by its capacity to compatibilize PA12 and the thermoplastic matrix.

## I. Introduction

Toughening of thermoplastics by a rubber is a very efficient strategy to overcome the brittleness of many engineering plastics.<sup>1</sup> However, the improvement of the fracture toughness is systematically accompanied by a drastic drop in modulus.<sup>2,3</sup> Therefore, a delicate compromise between toughness and stiffness has to be searched for. A core–shell morphology, which consists of a rigid core and a soft shell, has been proposed to impart a substantial toughening to the matrix while keeping rigidity reasonably high.<sup>3</sup> However, because of a lack of valuable models, no basic relationship between core–shell morphology and mechanical properties has ever been reported. The main reason is that the morphology of ternary polymer blends is primarily controlled by the spreading coefficients,<sup>3</sup> which limits the range of polymers that can build up a predetermined morphology. Moreover, for toughening to be efficient, there are specific requirements on the size and size distribution of the rubber particles.<sup>4</sup>

A possible strategy to develop a C–B core–shell morphology in a polymer matrix A consists of locating selectively an ABC triblock copolymer at the interface of a C in A dispersion. Depending on its interfacial activity, the triblock might accumulate at the interface, as a nonionic surfactant does.<sup>1b</sup> This ideal situation is shown in Scheme 1. As long as the A and C blocks are located in the parent phase, the ABC triblock is not only a compatibilizer for the C in A dispersion but also an encapsulating agent of the C domains. The thickness of the rubbery shell could then be tuned by the molecular weight of the central B block, whereas the core diameter is dictated by the C content and the capacity of the block copolymer to compatibilize C with A (thus to decrease the size of the dispersed domains). This type of morphology was reported by Fayt et al., who added a hydrogenated polybutadiene-*b*-polyisoprene-*b*-polystyrene to a polyethylene/polystyrene blend and observed

**Scheme 1. Encapsulation Strategy**



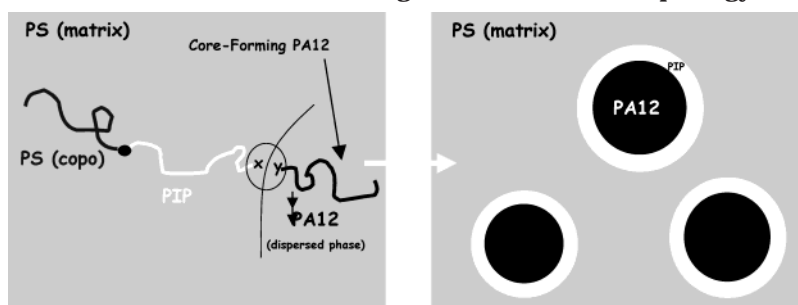
a polyisoprene shell around the polystyrene domains.<sup>5</sup> Similarly, Riess et al.<sup>6</sup> visualized the location of a PS-*b*-PIP-*b*-PMMA triblock in a PS/PMMA blend by the selective staining of PIP. Auschra and Stadler<sup>7</sup> added a PS-*b*-PEB-*b*-PMMA triblock to a PPE/SAN blend (where PEB and PPE stand for poly(ethylene-*co*-butylene) and poly(phenylene ether), respectively), to decrease the internal stress at the PS/PPE interface by the insertion of a PEB rubbery interphase. All the blends were prepared by solvent casting followed by annealing. Phase morphology was usually coarse, and the thickness of the rubber envelope was uneven.

This work aims at forming thermoplastic–PIP core–shell particles in a PS matrix by melt blending rather than by solvent casting. The limited control on the core–shell morphology in the aforementioned papers might have several origins. Depending on molecular weight and composition, the preformed triblock may have problems in diffusing to the interface for physical (melt viscosity<sup>8</sup>) and/or thermodynamic (competing micellization<sup>1,7</sup>) reasons. To tackle these problems and to have the triblock located at the interface as selectively and completely as possible, the strategy of forming the triblock copolymer in situ by reactive melt blending has been proposed and tested. For this purpose, a PS-*b*-PIP diblock end-capped by a phthalic anhydride at the PIP chain end has been synthesized and characterized.<sup>9</sup> It has been used as the reactive precursor of a PS-*b*-PIP-*b*-PA12 compatibilizing/encapsulating triblock for the

\* To whom correspondence should be addressed. E-mail: rjerome@ulg.ac.be.

<sup>†</sup> Current address: Atofina Research S.A., Zone Industrielle C, B-7181 Feluy, Belgium.

Scheme 2. Reactive Blending and Core–Shell Morphology



melt blending of a PS matrix and a polyamide (PA12) minor component (Scheme 2). As a result of the interfacial reaction between the diblock anhydride end group and the primary amine end group of PA12, the desired triblock is formed at the PS/PA12 interface, thus where it has to be for building up a core–shell morphology in PS.

## II. Experimental Section

**Materials.** Styrene (Sty; Aldrich, 99+%), isoprene (IP; Janssen Chimica, 99%), acrylonitrile (AN; Aldrich, 99+%), and ethylene oxide (EO; Meisser) were dried over  $\text{CaH}_2$  (Aldrich), distilled to remove the stabilizer, and stored under Ar at  $-20^\circ\text{C}$ . Cyclohexane was dried over  $\text{CaH}_2$  and distilled before use. Tetrahydrofuran (THF) was dried over Na/benzophenone and distilled before use. *s*-BuLi (Aldrich, 0.22 M in hexane), *n*-BuLi (Aldrich, 1 M in hexane), and triethylaluminum ( $\text{AlEt}_3$ ; Aldrich, 1 M in toluene) were used as received, or after dilution if required, and stored under Ar at  $-20^\circ\text{C}$ . Oligomers of styryllithium ( $\text{DP} = 3\text{--}4$ ; 1 M) were prepared by reaction of *s*-BuLi with styrene in toluene under Ar. Trimellitic anhydride chloride (TAC, Fluka, 99%) was stored and handled in a glovebox. Fluorenyllithium (1 M in toluene) was prepared by reaction of *s*-BuLi with fluorene (Aldrich) in toluene under Ar. CuBr (Aldrich) was purified by dispersion into acetic acid for 1 h, followed by filtration and washing with methanol, 1,1,4,7,10,10-hexamethyltriethylenetetraamine (HMTETA from Aldrich) was used in toluene (0.3 M), ammonium formate and Pd/C (both from Aldrich) were used as received, and dimethylformamide (DMF; from Aldrich) was dried for a week over  $\text{P}_2\text{O}_5$  (Aldrich) prior to distillation under reduced pressure. Liquids were transferred under argon (Ar; Meisser) with glass syringes or stainless steel capillaries, through rubber septa. Polyamide 12 was PA12 Rilsan AECHV0 from ATOFINA ( $M_n \approx 20000$  g/mol,  $M_w/M_n = 1.8$ ,  $[\text{NH}_2] = 25$   $\mu\text{equiv/g}$ , which means that only 50% of the chains are end-capped by one amino group, on average). Polystyrene (PS) was PS42K from BASF ( $M_n = 45000$  g/mol,  $M_w/M_n = 2$ ).

**Synthesis of (Co)polymers.** PS-*b*-PIP copolymers were prepared by sequential anionic polymerization of styrene and isoprene, initiated by *s*-BuLi. The polymerization reaction was terminated by either degassed methanol or oxirane. After acidification, the isolated PS-*b*-PIP-OH chains (oxirane deactivation) were reacted with trimellitic anhydride chloride to end-cap selectively the copolymer by a phthalic anhydride group as detailed elsewhere.<sup>9</sup>

Functional poly(styrene-*co*-acrylonitrile) (SAN-NH<sub>2</sub>) was prepared by atom transfer radical polymerization (ATRP). Briefly, 1-phenylethyl bromide was used as

initiator in the presence of CuBr/1,1,4,7,10,10-hexamethyltriethylenetetraamine in a 1/1 molar ratio. The SAN chains (70 wt % styrene) were systematically end-capped by a bromide, which was derivatized into an azide (by reaction with a large excess of sodium azide in DMF) followed by reduction into a primary amine with ammonium formate (catalyzed by Pd/C in DMF).<sup>9b,c</sup>

All the block copolymers were characterized by 400 MHz  $^1\text{H}$  NMR and SEC-UV.<sup>9b,10</sup> Size exclusion chromatography (SEC) was carried out in THF at  $40^\circ\text{C}$  with a HP1090 liquid chromatograph equipped with a HP1037A dual refractive index/UV detector (columns HP PL gel 5  $\mu\text{m}$ ,  $10^5$ ,  $10^4$ ,  $10^3$ , and  $100$  Å) calibrated with polystyrene standards (Polymer Labs). The flow rate was 1 mL/min.  $^1\text{H}$  NMR spectra were recorded with a Bruker AM 400 MHz spectrometer at  $25^\circ\text{C}$ .

**Polymer Blending.** Melt blending was carried out in a 5 cm<sup>3</sup> DSM microextruder at  $220^\circ\text{C}$  under nitrogen at 200 rpm for 2 min. The phase morphology remained unchanged beyond this blending time. PS was first added followed by the reactive diblock and the PA12 dispersed phase, respectively.

The phase morphology was observed with a Philips CM100 transmission electron microscope. A Reichert-Jung ultracryomicrotome equipped with a diamond knife was used to prepare ultrathin samples at  $-78^\circ\text{C}$ . The PIP phase was selectively stained with  $\text{OsO}_4$ . The morphology was observed in the direction perpendicular to the extrusion flow. The size of the dispersed phases was quantitatively analyzed with a computerized image analyzer (KS 100 Konton imaging system). A total of 200–300 dispersed domains were considered per sample. The cross-sectional surface area of these particles was converted to equivalent diameters by eqs 1 and 2. Because TEM micrographs were 2D slices through a 3D morphology,  $D$  was underestimated with an error of 10% or less.<sup>11</sup>

$$D_i = (4/\pi(\text{area}))^{0.5} \quad (1)$$

$$D_v = \sum n_i D_i^3 / \sum n_i D_i^2 \quad (2)$$

A JEOL JSM-840A scanning electron microscope (at 20 kV) was also used to observe fractured surfaces prepared at room temperature. Samples were coated by a 25 nm thick layer of Au/Pd alloy.

## III. Results and Discussion

PA12 chains are intrinsically end-capped by a primary amine highly reactive toward anhydride. Therefore, PS-*b*-PIP diblocks have been synthesized and end-capped by an anhydride on the PIP side (SIanh-1–3, Table 1). All these diblocks have comparable molecular weight but different composition and thus a different PIP block

**Table 1. Reactive Diblock Copolymers and Amino-Terminated SAN Synthesized in This Work**

code	type	$M_n$ ( $10^{-3}$ g/mol)	content	$M_w/M_n^a$	$f$ (%)
SIanh-1	PS- <i>b</i> -PIP-anh	30 (PS) <sup>a</sup> –5 (PIP) <sup>b</sup>	14% PIP	1.02	>85 <sup>c</sup>
SIanh-2	PS- <i>b</i> -PIP-anh	15 (PS) <sup>a</sup> –13 (PIP) <sup>b</sup>	46% PIP	1.03	>85 <sup>c</sup>
SIanh-3	PS- <i>b</i> -PIP-anh	3.5 (PS) <sup>a</sup> –26.5 (PIP) <sup>b</sup>	88% PIP	1.01	>85 <sup>c</sup>
SIanh-4	PS- <i>b</i> -PIP-anh	27 (PS) <sup>a</sup> –27 (PIP) <sup>b</sup>	50% PIP	1.05	>85 <sup>c</sup>
SAN-1 (30 wt % AN)	SAN-NH <sub>2</sub>	25		1.1	>75 <sup>d</sup>

<sup>a</sup> SEC with PS standards. <sup>b</sup> <sup>1</sup>H NMR (400 MHz) analysis of the triblock after purification. <sup>c</sup> Fraction of end-functional groups (anhydride) analyzed by 400 MHz <sup>1</sup>H NMR. <sup>d</sup> Fraction of end-functional groups (primary amine) analyzed by SEC-UV.<sup>9</sup>

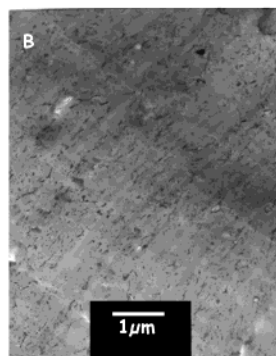
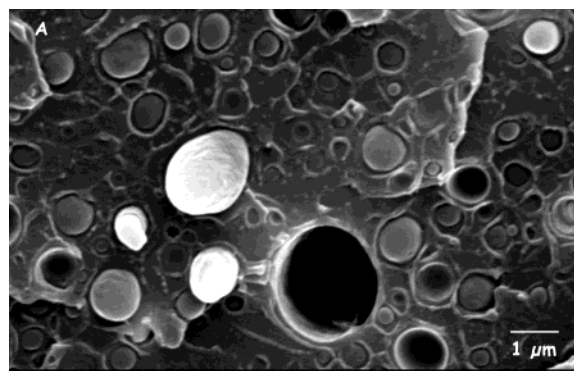


**Figure 1.** SEM micrograph of the fracture surface for a PS/PA12 (80/20) binary blend (A). TEM micrograph of a PS/PA12/PS-*b*-PIP (SIanh-1) ternary blend (80/10/10) (B).

length. They have been melt reacted with PA12 in the presence of a constant amount of PS (80 wt % ternary blends). The diblock/PA12 weight ratio has been changed from 75/20 to 50/50 and finally 25/75. First of all, the phase morphology of the PS/PA12 (80/20) binary blend has been analyzed by scanning electron microscopy (SEM) instead of TEM because of a lack of electronic contrast between the phases. Figure 1A shows a very coarse phase morphology without interfacial adhesion, typical of noncompatibilized immiscible blends.<sup>1</sup> To make a second reference blend available, a nonreactive ternary blend (PS/PA12/diblock = 80/10/10) has been prepared, in which the diblock forms micelles in the PS matrix and does not encapsulate the PA12 domains (TEM; Figure 1B).

As far as the reactive blends are concerned, diblocks with a PIP block of different lengths have been considered to validate the concept of a PIP shell with a thickness controlled by the PIP molecular weight. For each diblock copolymer, several blends have been prepared by changing the diblock/PA12 weight ratio, keeping in mind the tuning of the core diameter. The total content of PA12 + diblock is maintained at 20%.

**PS-Rich Reactive Precursor.** Compared to the PS/PA12 (80/20) reference blend, 25 wt % PA12 has been substituted by a reactive PS-*b*-PIP-anh diblock that

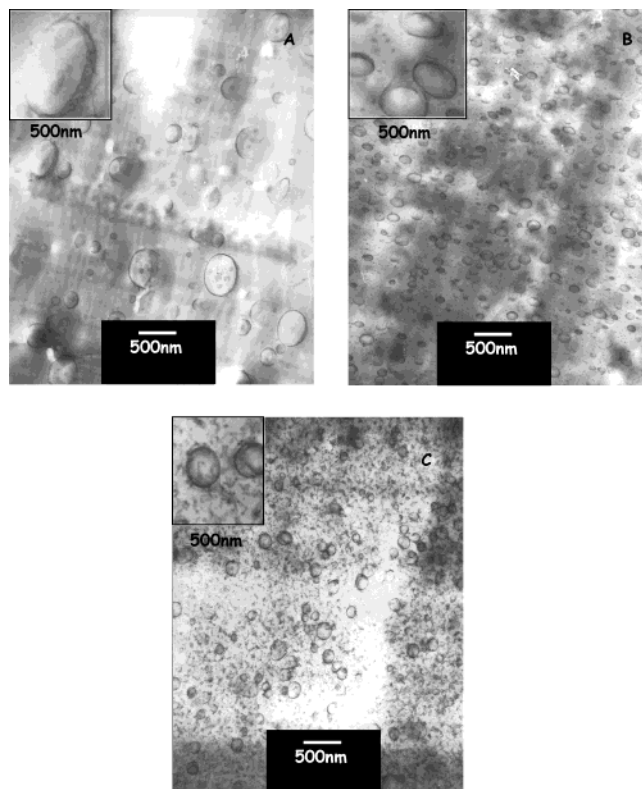
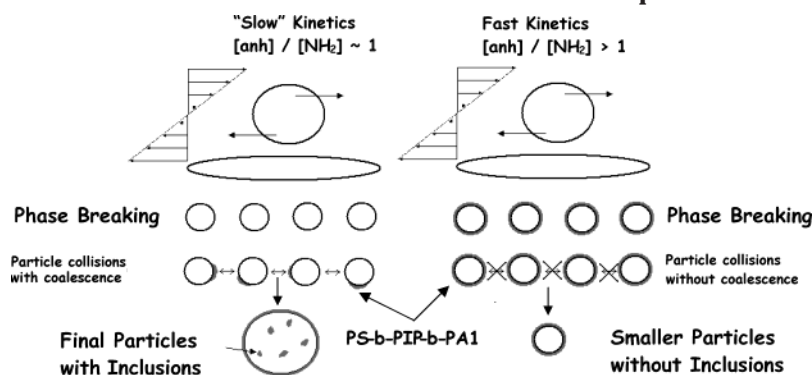


**Figure 2.** TEM micrographs for the PS/PA12/SIanh-1 (80/15/5) reactive blend (A), the PS/PA12/SIanh-1 (80/10/10) reactive blend (B), and the PS/PA12/SIanh-1 (80/5/15) reactive blend (C).

contains 14 wt % PIP (SIanh-1, Table 1). A drastic decrease in the size of the PA12 domains is observed, as result of conversion of the diblock into a triblock (Figure 2A). Moreover, the selective staining of the PIP block by OsO<sub>4</sub> shows a continuous rubbery layer around the dispersed phases. PA12 particles with a diameter in the 400 nm range are thus encapsulated by the in situ formed triblock. This very first experiment is encouraging evidence that the reactive blending is an efficient strategy for building up a core-shell morphology. A 2-fold increase in the SIanh-1 content results in a further decrease in the average particle size from 400 to 200 nm. The thickness of the PIP shell is unchanged, consistent with encapsulation of PA12 by a monolayer of the triblock formed by reactive blending ( $M_n$  of PIP is constant). That the core diameter of the dispersed particles has decreased is the expected consequence of a lower content of PA12 and a comparatively larger amount of copolymer instantaneously formed in situ. In the same vein, occlusions are observed in the PA12 cores in Figure 2A, which is the signature of particle coalescence during blending (Scheme 3).<sup>12</sup> This phenomenon does not occur anymore, when the relative amount of diblock is increased (Figure 2B). Indeed, when the



## Scheme 3. Occlusions of the Matrix in the PA12 Dispersed Phase



amount of diblock is increased from 25 to 50 wt % of the dispersed phase, the amine/anhydride molar ratio is decreased from 3.0 to 1.0; thus, the reactive system is shifted from an excess of amino-end-capped PA12 to the reaction stoichiometry, the nonreactive PA12 chains (50% of the added amount) being then the core-forming material. A further increase in the relative content of the diblock in the dispersed phase (75 wt %) expectedly has no significant impact on the phase morphology, because the additional copolymer chains are in excess with respect to the amine-containing PA12. Figure 2C accordingly shows PA12 particles with an average diameter of 200 nm, completely encapsulated by a PIP shell. The dependence of the volume-to-surface average particle diameter ( $D_v$ ; eq 2) on the copolymer content in the dispersed phase is shown in Figure 3, which confirms that, beyond 50 wt % reactive diblock in the dispersed phase,  $D_v$  is constant. In parallel, the excess of diblock accumulates in the PS matrix as observed in Figure 2C, consistent with the morphology of a binary blend of the nonreactive PS-*b*-PIP copolymer with the PS matrix (Figure 4). Comparison of parts A and B of Figure 2 supports that the efficiency of the PS/PA12 compatibilization is improved when a larger amount of triblock is instantaneously formed in situ. This kinetic effect accounts for a faster and more complete encapsulation of the PA12 particles formed by shear-breaking.<sup>12</sup> Scheme 3 tentatively illustrates the balance between phase breaking and phase coalescence in relation to the amount of block copolymer made available in the system, together with the final morphology of the dispersed phases. This first series of experiments

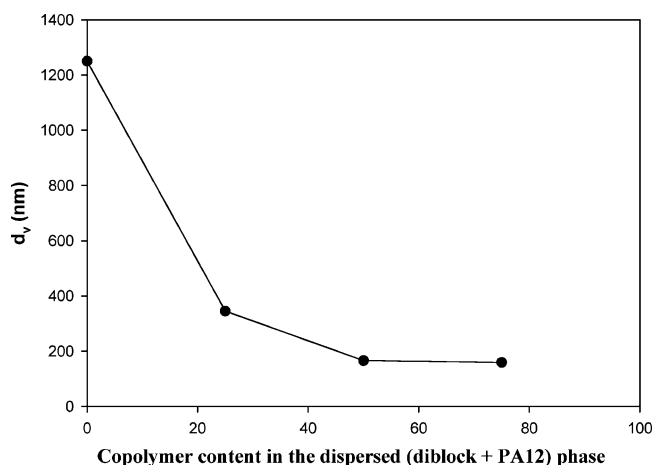


**Figure 3.** Dependence of the volume-average diameter,  $D_v$ , for the PA12/PIP core-shell objects on the diblock content of the dispersed phase.

confirm that changing the blend composition (i.e., the PA12/copolymer ratio) is a way to tune the balance of particle size (i.e., toughness) and amount of rubber (i.e., stiffness).

**Symmetric Reactive Precursor.** The molecular weight of the PIP block has been increased from 5000 to 13000 while keeping constant that of the diblock. Substitution of S1anh-2 for S1anh-1 (Table 1) in the PS/PA12/S1anh (80/15/5) blend does not change the phase morphology including the particle diameter and occlusions in the dispersed phases (Figure 5A). There is however a difference in the shell thickness, which is the expected consequence of the higher molecular weight of the PIP block. This characteristic feature has not been quantified because it depends on several poorly controlled experimental parameters, such as staining conditions, angle between microtoming direction and interface, film thickness, beam damage, etc. The same conclusion holds for the 80/10/10 ternary blend (Figure 5B). However, when the diblock content in the dispersed binary phase is increased further (75 wt %), a multi-layered shell is observed around the PA12 cores (Figure 5C). This observation is actually consistent with the lamellar morphology of the neat symmetric diblock and its macrophase separation when blended with the PS matrix.<sup>13</sup> At this blend composition, the excess of reactive diblock (cf. supra) phase separates as easily as the system is in the dry brush regime,<sup>13,14</sup> the "mono-disperse" PS block being of lower molecular weight than the polydisperse PS matrix. Figure 5D is a magnification of core-multilayer shell nanoobjects. Clearly, the unreacted copolymer preferentially locates at the shell/matrix interface with formation of an onion-like structured shell in relation to the diblock excess. The extreme situation of the aggregation of two core-shell

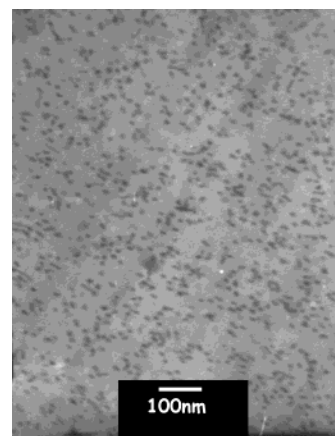


**Figure 4.** TEM micrograph for the PS/S1anh-1 (80/20) blend.

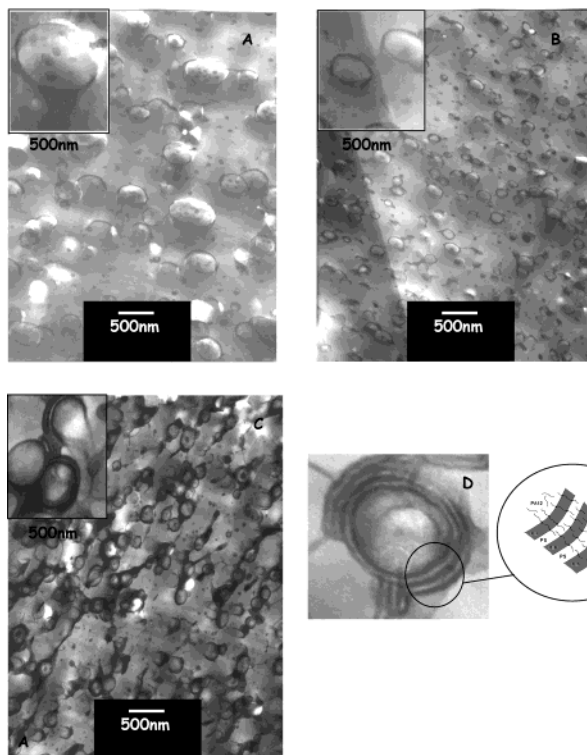


**Figure 5.** TEM micrographs for the PS/PA12/Sianh-2 (80/15/5) reactive blend (A), the PS/PA12/Sianh-2 (80/10/10) reactive blend (B), the PS/PA12/Sianh-2 (80/5/15) blend (C), the blend in (C) at higher magnification (D).

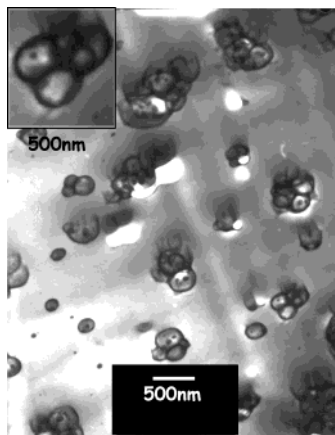


**Figure 6.** TEM micrograph for the PS/PA12/Sianh-3 (80/15/5) reactive blend.

particles as a result of a common multilayered envelope is observed in the inset of Figure 5C.

**PIP-Rich Reactive Precursor.** Finally, the Sianh-3 reactive diblock with a very short PS block (Table 1) has been melt blended with 80% PS and 15% PA12. The aggregation of core-shell particles is dominant (Figure 6). The steric stabilization by the PS block is no longer effective enough to maintain the individual core-shell particles far away one from each other. Similarly, the diblock copolymer forms micrometer-sized phases when blended with the PS matrix. A change in the composition of the dispersed phase in the ternary blend did not expectedly improve the situation. Nevertheless, the concept of the tuning of the shell thickness by the molecular weight of the central PIP block is validated as illustrated in Figure 7. The shell thickness is directly compared for the PIP blocks of extreme molecular

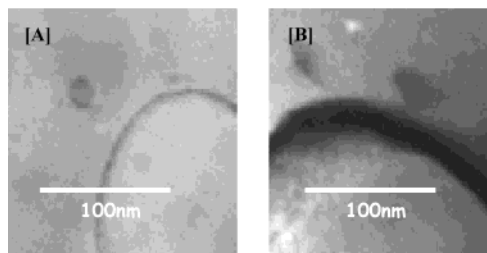


**Figure 7.** Qualitative comparison of the shell thickness of the core-shell nanoobjects formed by the PS/PA12/Sianh-1 (80/15/5) reactive blend (A) and the PS/PA12/Sianh-3 (80/15/5) reactive blend (B).

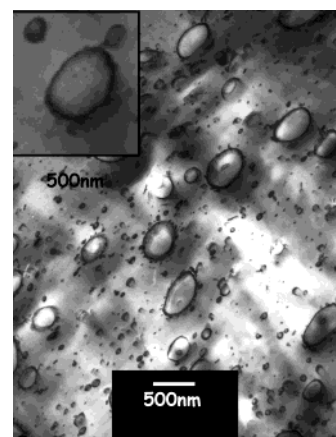


**Figure 8.** TEM micrograph for the PS/PA12/Sianh-4 (80/15/5) reactive blend.

weight, i.e., 5000 (Sianh-1) and 26000 (Sianh-3). Although it might be argued that the larger thickness of the PIP shell in Figure 7B results from the accumulation of unreacted Sianh-3 diblock at the interface, it must be noted that the reaction of Sianh-1 and Sianh-2 copolymers of quite comparable molecular weight at the same composition (25 wt % of the dispersed phase) under the same experimental conditions is close to completion as assessed by the absence of unreacted diblocks in the PS phase (comparison of parts A and C of Figure 2, for Sianh-1) and of multilayered shells (comparison of parts A and C of Figure 5, for Sianh-2). Therefore, there is no reason for Sianh-3 to be an exception in terms of complete conversion in the 80/15/5 ternary blends. So, Figure 7 shows that it is possible to change the shell thickness, which, in conjunction with the control of the core diameter (by the PA12 content), meets the requirement for a model system suited to the analysis of the deformation mechanisms of core-shell-modified thermoplastics.

**Coalescence Inhibition.** Until now, the total molecular weight of the reactive diblock has been kept essentially unchanged. Although a rather large PIP shell was developed by the Sianh-3 copolymer, the core-shell particles then spontaneously formed aggregates. An increase in the PS molecular weight at constant PIP length ( $M_n = 26500$  g/mol) is a way to solve the problem, because a larger interfacial brush is a requirement for effective steric stabilization.<sup>8</sup> The Sianh-4 reactive diblock copolymer (Table 1) has accordingly been synthesized. The expectation of homogeneously dispersed individual core-shell particles has been confirmed, as illustrated in Figure 8.

**Extension to Reactive Polymers Other than PA12.** The general character of the strategy developed

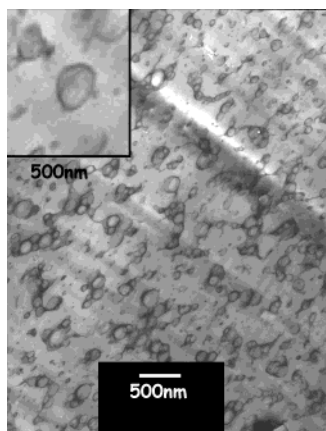


**Figure 9.** TEM micrograph for the PS/SAN/SIanh-2 (80/10/10) reactive blend.

in this work has been supported by the successful substitution of the core-forming PA12 by a primary-amine-end-capped styrene/acrylonitrile (SAN-1) copolymer. No drastic change in morphology is observed (Figure 9).

#### IV. Conclusions

A model system based on two thermoplastics, a PS matrix and PA12 dispersed phases in conjunction with a rubber (PIP), has been developed with the purpose to disperse homogeneously core-shell particles in PS. The basic strategy relies on the selective location of a PS-*b*-PIP-*b*-PA12 triblock copolymer at the PS/PA12 interface. Formation of a PS-*b*-PIP-*b*-PA12 triblock in PS by reactive blending of an end-functional PS-*b*-PIP diblock (reactivity on PIP) with partly reactive PA12 leads to the encapsulation of the dispersed PA12 phases by a PIP shell. Unreacted diblock (used in excess) forms micelles in one phase or mesophases at the interface, depending on the molecular weight and composition. The key observation is that the thickness of the PIP shell is easily modified by the molecular weight of the PIP block. The PA12 core diameter can also be tuned by changing the molar excess of PA12 with respect to the reactive diblock copolymer. The reactive blending strategy is general enough for using completely different reactive core-forming thermoplastics, e.g., a semicrystalline polyamide vs an amorphous SAN copolymer. It is now possible to make model polyblends available for investigating the impact of crucial parameters, such as

particle diameter, shell thickness, and nature of the core, on the deformation mechanism and the ultimate mechanical properties of rubber-toughened thermoplastics.

**Acknowledgment.** We are very indebted to the Belgian Science Policy for support in the frame of Grant PAI V/03, "Supramolecular Chemistry and Supramolecular Catalysis". We are grateful to Dr. C. Pagnoulle and Dr. Z. Yin for fruitful discussions. C.K. is an "Aspirant" fellow by the Fonds National de la Recherche Scientifique.

#### References and Notes

- (1) (a) Bucknall, C. *Thoughened Plastics*; Applied Sciences: London, 1977. (b) Koning, C.; Van Duin, M.; Pagnoulle, C.; Jérôme, R. *Prog. Polym. Sci.* **1998**, *23*, 707 and references therein.
- (2) Kerner, E. H. *Proc. Phys. Soc.* **1956**, 69B, 808.
- (3) (a) Hobbs, S. Y.; Dekkers, M. E. J.; Watkins, V. H. *Polymer* **1988**, *29*, 1598. (b) Nemirovski, N.; Siegmund A.; Narkis, N. *J. Macromol. Sci., Phys.* **1995**, *34B*, 459. (c) Horiuchi, S.; Matchariyakul, N.; Yase, K.; Kitano, T.; Choi, H. K.; Lee, Y. M. *Polymer* **1996**, *37*, 3065. (d) Horiuchi, S.; Matchariyakul, N.; Yase, K.; Kitano, T.; Choi, H. K.; Lee, Y. M. *Polymer* **1997**, *38*, 59. (e) Rösch, J. *Polym. Eng. Sci.* **1995**, *35*, 1917. (f) Luzinov, I.; Xi, K.; Pagnoulle, C.; Huynh-Ba, G.; Jérôme, R. *Polymer* **1999**, *40*, 2511. (g) Luzinov, I.; Pagnoulle, C.; Jérôme, R. *Polymer* **2000**, *41*, 3381. (h) Luzinov, I.; Pagnoulle, C.; Jérôme, R. *Polymer* **2000**, *40*, 7099.
- (4) Argon, A. S.; Cohen, R. E. *Polymer*, in press.
- (5) Fayt, R.; Jérôme, R.; Teyssié, Ph. *J. Polym. Sci., Polym. Lett. Ed.* **1986**, *24*, 25.
- (6) (a) Riess, G.; Schlienger, M.; Marti, S. *J. Macromol. Sci.* **1980**, *B17*(2), 355. (b) Schlienger, M. Ph.D. Thesis, Mulhouse, 1976.
- (7) Auschra, C.; Stadler, R. *Macromolecules* **1993**, *26*, 6364.
- (8) Karim, A.; Douglas, J.; Satija, S.; Han, C.; Goyette, R. *Macromolecules* **1999**, *32*, 1119.
- (9) (a) Koulic, C.; Yin, Z.; Pagnoulle, C.; Jérôme, R. *Angew. Chem., Int. Ed.* **2002**, *41*, 2154. (b) Koulic, C. Ph.D. Thesis, University of Liège, 2004. (c) Koulic, C.; Jérôme, R. *Macromolecules* **2004**, *37*, 888.
- (10) Koulic, C.; Jérôme, R. *Macromolecules*, in press.
- (11) Macosko, C.; Guegan, P.; Khandpur, A.; Nakayama, A.; Marechal, P.; Inoue, T. *Macromolecules* **1996**, *29*, 5590.
- (12) (a) Pagnoulle, C.; Koning, C.; Leemans, L.; Jérôme, R. *Macromolecules* **2000**, *33*, 6275. (b) Pagnoulle, C.; Jérôme, R. *Macromolecules* **2001**, *34*, 965. (c) Pagnoulle, C. Ph.D. Thesis, University of Liege, 1999.
- (13) (a) Kinning, D. J.; Winey, K.; Thomas, E. L. *Macromolecules* **1988**, *21*, 3502. (b) Kinning, D. J.; Thomas, E. L.; Fetters, L. J. *J. Chem. Phys.* **1989**, *90*, 5806. (c) Kinning, D. J.; Winey, K.; Thomas, E. L. *Macromolecules* **1991**, *24*, 3893.
- (14) Leibler, L. *Makromol. Chem., Macromol. Symp.* **1988**, *16*, 1.

MA035826A